Semiclassical initial value representation study of internal conversion rates

Reuven Ianconescu and Eli Pollak[a]

Chemical Physics Department, Weizmann Institute of Science, 76100, Rehovoth, Israel

(Dated: August 12, 2018)

Abstract

Internal conversion is an inherently quantum mechanical process. To date, "on the fly" computation of internal conversion rates is limited to harmonic approximations, which would seem to be especially unsuitable, given that the typical transition to the ground electronic state occurs at energies which are far from the harmonic limit. It is thus of interest to study the applicability of the SemiClassial Initial Value Representation (SCIVR) approach which is in principle amenable to "on the fly" studies even with "many" degrees of freedom. In this paper we study the applicability of the Herman-Kluk (HK) SCIVR to a model system with two coupled and anharmonic degrees of freedom. We find that (a) The HK SCIVR is a good approximation to the exact quantum dynamics; (b) Computation of the first order correction to the HK-SCIVR approximation corroborates the accuracy; (c) By studying a large parameter range, we find that the harmonic approximation is mostly unsatisfactory; (d) For the specific model used, the coupling between the modes was found to be relatively unimportant. These results imply that the HK-SCIVR methodology is a good candidate for "on the fly" studies of internal conversion processes of "large" molecules.

[a] email: eli.pollak@weizmann.ac.il

PACS numbers:

I. INTRODUCTION

The theory of nonradiative decay of excited vibronic states of molecules has a long history. Almost fifty years ago, Robinson and Frosch [1, 2] and some years later, Lin and Bersohn [3, 4] set the framework in their seminal papers. A summary of the historical development of the theory may be found in a recent review by Lin et al [5]. More recently, Peng et al [6] have adapted the Green's function method for the computation of internal conversion rates. This has led to the computation of internal conversion rates of large molecules, using ab-initio force fields for both the electronically excited and ground states [6–8]. These studies are limited though to harmonic models for the vibrations in both the ground and excited electronic state [9]. At best, anharmonicity is dealt with using perturbation theory about the harmonic limit as described for example in Refs. [10–12]. Especially for Internal Conversion (IC), where the transition occurs from an excited electronic state to high energy vibrations in the ground electronic state, one may expect that the harmonic approximation for the dynamics and its extensions on the ground state potential may fail since the density of vibrational states on the ground electronic state would be typically much higher than predicted from a harmonic model.

An important advantage of the harmonic theory is that one may use ab-initio methods for the force fields and thus estimate from first principles the IC rates [7, 8, 11, 12]. Numerically exact computations for the dynamics of systems with up to 100 coupled degrees of freedom are possible today, using the MultiConfiguration Time Dependent Hartree (MCTDH) method [13]. However, such computations necessitate a global description of the potential energy surface and so are still difficult to implement from first principles. A compromise approach would be to use the SemiClassial Initial Value Representation (SCIVR) approach [14]. SCIVR is known to treat quantum effects such as zero point energy, superposition and weak to moderate tunneling rather well. Especially the Herman-Kluk (HK) frozen Gaussian SCIVR propagator [15] is amenable to ab-initio computations in the sense that it relies on the dynamics of the bare potential and needs as input local force field information only. It is thus of interest to test the HK SCIVR approximation for the computation of internal conversion rates, under a variety of conditions. If one finds that the approximation is "good" then one may hope to implement it "on the fly" and thus provide a more accurate description of internal conversion.

The central objectives of this paper are (a) to test the applicability of the HK SCIVR approximation to IC by comparing it with numerically exact quantum results; (b) to explore the relevant parameter space which is expected to affect the IC rates and compare the correct anharmonic IC transition probabilities with those obtained with a harmonic approximation of the ground state potential. We use a model system with 2 degrees of freedom for which it is not difficult to compute the numerically exact quantum results. It is also of interest to study some qualitative effects on the internal conversion process. For example, Henke et al [16] found that increasing the energy of the initial vibrational state in the excited electronic state will increase the IC rate. The influence of the initial vibronic state has been investigated experimentally by Frisoli et al [17] for the formaldehyde molecule. With this in mind, we have studied in some detail how variations in the force field as well as the preparation of the system in the excited electronic state affect the IC rate and how well this is approximated by the HK SCIVR method.

In Sec. II we review the formalism needed for the computation of the radiationless decay rate as well as the relevant SCIVR formulae needed for implementation. Computations on a model system with two degrees of freedom, used in the past to model water and carbon dioxide are presented in Section III. Comparison of the HK SCIVR method with numerically exact quantum results is encouraging, as the two are almost identical. A first order perturbation theory correction of the HK SCIVR [18, 19] is found to be very small. We end with some concluding remarks in Sec. IV.

II. FORMALISM

A. Theory of radiationless decay

We consider the decay of an excited vibronic state, via nonadiabatic coupling to the ground electronic state. The potentials involved are drawn schematically in Fig. 1. The excited state potential is shifted in energy (ΔE) relative to the ground state and its equilibrium position is shifted by Δq relative to the ground state minimum.

The radiationless decay from an excited vibronic state to the ground electronic state is

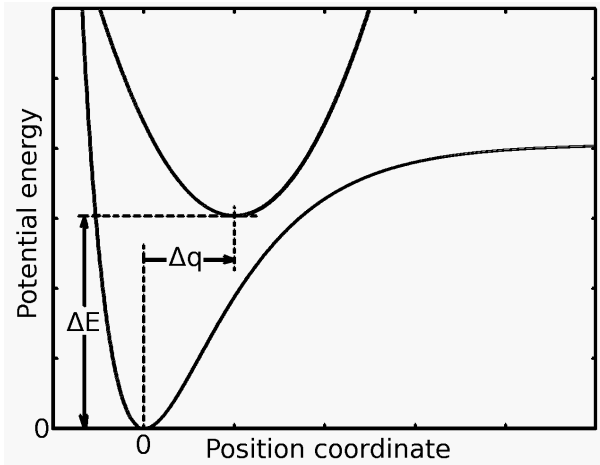

FIG. 1: Adiabatic surfaces describing the ground and excited electronic states in one dimension. Δq is the spatial shift between the surfaces, it is defined as positive if the shift is towards the dissociative side of the ground state and negative if it is towards the repulsive side. ΔE is the energy gap between the bottom of the ground and excited electronic states.

given by Fermi's golden rule [4, 6]:

$$W_{i\to f} = \frac{2\pi}{\hbar}\sum_{\nu}\sum_{\nu'} P_{\nu'}|\langle\phi_\nu|H_{\rm BO}|\psi_{\nu'}\rangle|^2\delta(E_\nu - E_{\nu'}) \tag{2.1}$$

where $P_{\nu'}$ is the initial probability of the molecule to be in the ν' energy level of the excited electronic state whose eigenfunction is $\psi_{\nu'}$. The final state ν on the ground electronic surface has the energy E_ν and eigenfunction ϕ_ν. Energy conservation is reflected through the Dirac "delta" function $\delta(E_\nu - E_{\nu'})$. $H_{\rm BO}$ is the Born-Oppenheimer coupling operator due to the breakdown of the adiabatic approximation and is expressed by a sum of nuclear momenta operating on the nuclear and electronic wave functions as follows [4, 6, 10, 20]

$$H_{\rm BO}|\psi\chi\rangle = \sum_{l}\frac{1}{m_l}\left(-i\hbar\frac{\partial}{\partial q_l}|\psi\rangle\right)\left(-i\hbar\frac{\partial}{\partial q_l}|\chi\rangle\right) \tag{2.2}$$

where the sum is over all degrees of freedom, and $|\psi\rangle$ and $|\chi\rangle$ are the nuclear and the electronic wave functions respectively.

The central thrust of this paper is to study the dynamics on the ground electronic state potential. We assume that the electronic matrix element can be obtained from ab-initio computations and so will henceforth treat it as a constant $C_l \equiv \langle\chi|\left(-i\hbar\frac{\partial}{\partial q_l}\right)|\chi\rangle$ which has

the dimensions of momentum. The nonadiabatic coupling operator may then be written as:

$$H_{\mathrm{BO}} = \sum_l \frac{C_l}{m_l}\left(-i\hbar\frac{\partial}{\partial q_l}\right) \tag{2.3}$$

and it now operates only on the nuclear wavefunction. Assuming that the initial state is specified with unit probability and energy E, allows to omit the sum on ν' so that after using Eq. (2.3) we obtain:

$$W_{i\to f} = 2\pi\hbar\sum_l\left(\frac{C_l}{m_l}\right)^2\sum_\nu |\langle\phi_\nu|\partial\psi/\partial q_l\rangle|^2\delta(E_\nu - E) \tag{2.4}$$

where E is the energy of the initial excited state, represented by the wavefunction ψ.

To further simplify, we specify our model Hamiltonian which is based on a small molecule such as H_2O, where the two outer atoms are equal [21, 22]. The ground electronic state nuclear Hamiltonian may be described by two degrees of freedom which are coupled through a momentum term, while the bond potentials are Morse potentials:

$$H_g = \frac{p_1^2}{2m_1} + \frac{p_2^2}{2m_2} + \frac{p_1p_2}{M} + D_1[1-\exp(-\alpha_1 q_1)]^2 + D_2[1-\exp(-\alpha_2 q_2)]^2 \tag{2.5}$$

Typically, in the excited electronic state, the system is prepared at low energies where a harmonic approximation for the motion is reasonable. The nuclear Hamiltonian for the excited electronic state is thus approximated as:

$$H_e = \frac{p_1^2}{2m_1} + \frac{p_2^2}{2m_2} + \frac{1}{2}m_1\omega_1^2(q_1-\Delta q_1)^2 + \frac{1}{2}m_2\omega_2^2(q_2-\Delta q_2)^2 + \Delta E \tag{2.6}$$

where ω_1 and ω_2 are the harmonic frequencies of the excited energy surface, Δq_1 and Δq_2 are the coordinate shifts between the excited and ground electronic state surfaces, and ΔE is the energy gap (see Fig. 1). This model is symmetric with respect to the middle atom, so that the masses are equal $m = m_1 = m_2$. We may therefore also assume that the nonadiabatic coupling constants are equal $C = C_1 = C_2$. This allows us to define a *dimensionless* transition probability as $P_{i\to f} = \hbar m W_{i\to f}/C^2$ obtaining:

$$P_{i\to f} = 2\pi\hbar^2\sum_l\frac{1}{m_l}\sum_\nu |\langle\phi_\nu|\partial\psi/\partial q_l\rangle|^2\delta(E_\nu - E). \tag{2.7}$$

In principle, this transition probability is discrete since the initial energy in the excited system takes on only discrete values. Only if there exists a state on the ground potential surface whose energy $E_\nu = E$ will a transition be possible. However, when the density of states is high, we practically measure the average decay into a continuum of states. Let us define $\sigma(E)$ as the mean interval between successive vibrational states in the ground electronic state at the energy E (for further details see the Appendix). The mean interval is inversely proportional to the density of states and so is typically larger at low energies and decreases as one moves up the vibrational ladder of states. The transition probability may then be coarse grained by "smearing" the Dirac "delta" function with a Gaussian of width $\sigma(E)$:

$$\delta(E_\nu - E) \simeq \frac{1}{\sqrt{2\pi\sigma}} e^{-\frac{(E_\nu - E)^2}{2\sigma^2}} = \frac{1}{2\pi\hbar} \int_{-\infty}^{\infty} dt\ e^{-\frac{i}{\hbar}(E_\nu - E)t} e^{-\frac{t^2\sigma^2}{2\hbar^2}} \tag{2.8}$$

where the dependence of σ on E has been omitted for the sake of brevity. Substituting Eq. (2.8) into Eq. (2.4) and using the definition of the propagator for the evolution on the ground electronic state we readily obtain that the expression for the transition probability is:

$$P_{i\to f} = \hbar \sum_l \frac{1}{m_l} \int_{-\infty}^{\infty} dt\ e^{\frac{i}{\hbar}Et} e^{-\frac{t^2\sigma^2}{2\hbar^2}} \langle \partial\psi/\partial q_l | e^{-\frac{i}{\hbar}H_g t} | \partial\psi/\partial q_l \rangle \tag{2.9}$$

We are interested in computing the transition probability as a function of the energy gap ΔE and the initial vibrational state in the excited electronic state. Denoting the initial wavepacket associated with the n, m eigenvalue of H_e (with n, m referring to coordinates 1 and 2 respectively) as $\psi \equiv \psi_{nm}$, the energy relative to the bottom of the excited surface (see Figure 1) is $\hbar\omega_1(n + 1/2) + \hbar\omega_2(m + 1/2)$ so that the energy E in (2.9), is

$$E = \Delta E + \hbar\omega_1(n + 1/2) + \hbar\omega_2(m + 1/2). \tag{2.10}$$

Defining the time dependent overlap

$$\rho_{nm}(t) \equiv \hbar \sum_l \frac{1}{m_l} \langle \partial\psi_{nm}/\partial q_l | e^{-\frac{i}{\hbar}H_g t} | \partial\psi_{nm}/\partial q_l \rangle, \tag{2.11}$$

noting that the mean energy interval function $\sigma(E)$ is a slowly varying function of the

energy so that

$$\sigma(E) = \sigma(\Delta E + \hbar\omega_1(n+1/2) + \hbar\omega_2(m+1/2)) \equiv \sigma_{mn}, \tag{2.12}$$

we finally have that the transition probability is a Fourier transform of the overlap function:

$$P_{n,m\to f} = \int_{-\infty}^{\infty} dt \ \exp\left[\frac{i}{\hbar}(\Delta E + \hbar\omega_1(n+1/2) + \hbar\omega_2(m+1/2))t\right] \exp\left(-\frac{\sigma_{mn}^2 t^2}{2\hbar^2}\right) \rho_{nm}(t). \tag{2.13}$$

We remark that in the model system with two degrees of freedom studied in this paper one cannot distinguish clearly between the initial decay of the wavepacket and fractional revivals of it. Therefore, the relevant time scale during which the integrand takes on meaningful values is $\pm\frac{\hbar}{\sigma_{mn}}$, so that the higher the density of states on the ground electronic surface, the longer one needs to determine the quantum dynamics. This may present a challenge to the accuracy of the semiclassical approximation described below. However, when the number of degrees of freedom increases significantly, one expects only the initial decay to be meaningful, so that as the density of states increases, the integration time should *decrease* making it easier to implement a semiclassical approach.

B. The semiclassical Herman-Kluk propagator

The Herman Kluk SCIVR propagator for a system with N degrees of freedom is [15]

$$\hat{K}_0(t) = \int_{-\infty}^{\infty} \frac{d\mathbf{p}d\mathbf{q}}{(2\pi\hbar)^N} R(\mathbf{p},\mathbf{q},t) \exp\left(\frac{i}{\hbar}S(\mathbf{p},\mathbf{q},t)\right) \ |g(\mathbf{p},\mathbf{q},t)\rangle\langle g(\mathbf{p},\mathbf{q},0)| \tag{2.14}$$

where $\mathbf{p}$ and $\mathbf{q}$ are the N dimensional momentum and coordinate variables respectively. The Herman Kluk prefactor is defined as:

$$R(\mathbf{p},\mathbf{q},t) = \sqrt{\det\left[\frac{1}{2}\left(\mathbf{\Gamma}^{1/2}\mathbf{M}_{qq}\mathbf{\Gamma}^{-1/2} + \mathbf{\Gamma}^{-1/2}\mathbf{M}_{pp}\mathbf{\Gamma}^{1/2} - i\hbar\mathbf{\Gamma}^{1/2}\mathbf{M}_{qp}\mathbf{\Gamma}^{1/2} + \frac{i}{\hbar}\mathbf{\Gamma}^{-1/2}\mathbf{M}_{pq}\mathbf{\Gamma}^{-1/2}\right)\right]}. \tag{2.15}$$

The monodromy matrices are denoted

$$\mathbf{M}_{ab} \equiv \frac{\partial \mathbf{a}_t(\mathbf{p},\mathbf{q})}{\partial \mathbf{b}} \tag{2.16}$$

where $\mathbf{a}$ and $\mathbf{b}$ may be either $\mathbf{p}$ or $\mathbf{q}$, and $\mathbf{\Gamma}$ is a constant in time $N \times N$ matrix (usually taken to be diagonal), establishing the width of the coherent states - see Eq. (2.18). Each initial phase space point $\mathbf{p},\mathbf{q}$ is evolved classically reaching the point $\mathbf{p}_t,\mathbf{q}_t$ at time t. The classical action along the trajectory is

$$S(\mathbf{p},\mathbf{q},t) = \int_0^t dt' \left(\mathbf{p}'_t \dot{\mathbf{q}}'_t - H(\mathbf{p},\mathbf{q})\right) \tag{2.17}$$

and the coherent state matrix element $|g\rangle$ in the coordinate representation is given by

$$\langle \mathbf{x}|g(\mathbf{p},\mathbf{q},t)\rangle = \left(\frac{\det(\Gamma)}{\pi^N}\right)^{1/4} \exp\left[-\frac{1}{2}(\mathbf{q}_t-\mathbf{x})^{\mathrm{T}}\mathbf{\Gamma}(\mathbf{q}_t-\mathbf{x}) + \frac{i}{\hbar}\mathbf{p_t}\cdot(\mathbf{x}-\mathbf{q}_t)\right]. \tag{2.18}$$

The HK propagator as defined in Eq. (2.14) may be considered to be a zero-th order approximation to the exact quantum propagator $\exp\left(-\frac{i}{\hbar}Ht\right)$. As has been shown in Refs. [18, 19] higher order corrections to the propagator may be calculated with the aid of the recursion relation:

$$\hat{K}_{j+1}(t) = \frac{i}{\hbar}\int_0^t dt' \hat{K}_j(t-t')\hat{C}(t') \tag{2.19}$$

where the correction operator $\hat{C}(t)$ is given by

$$\hat{C}(t) = \int_{-\infty}^{\infty} \frac{d\mathbf{p}d\mathbf{q}}{(2\pi\hbar)^N} R(\mathbf{p},\mathbf{q},t) \exp\left(\frac{i}{\hbar}S(\mathbf{p},\mathbf{q},t)\right) \widehat{\Delta V}(\hat{\mathbf{q}},\mathbf{p},\mathbf{q},t)|g(\mathbf{p},\mathbf{q},t)\rangle\langle g(\mathbf{p},\mathbf{q},0)| \tag{2.20}$$

and $\widehat{\Delta V}(\hat{\mathbf{q}},\mathbf{p},\mathbf{q},t)$ is the potential difference operator, which has different forms for different semiclassical representations [23]. For the HK representation the potential difference operator is

$$\widehat{\Delta V}(\hat{\mathbf{q}},\mathbf{p},\mathbf{q},t) = V(\mathbf{q}_t) + \nabla V(\mathbf{q}_t)\cdot(\hat{\mathbf{q}}-\mathbf{q}_t) - \frac{\hbar^2}{2}\mathrm{Tr}(\Gamma) + \frac{\hbar^2}{2}(\hat{\mathbf{q}}-\mathbf{q}_t)^{\mathrm{T}}\mathbf{\Gamma}^2(\hat{\mathbf{q}}-\mathbf{q}_t) - V(\hat{\mathbf{q}}) + i\hbar\frac{\dot{R}(\mathbf{p},\mathbf{q},t)}{R(\mathbf{p},\mathbf{q},t)}. \tag{2.21}$$

III. NUMERICAL RESULTS

A. The quality of the HK SCIVR approximation for the IC transition probability

For all the calculations we employed the potential parameters used previously for H_2O as given in Refs. [21, 22]. The effective masses m_1 and m_2 are $\frac{16}{17}$ of the proton mass, however the coupling mass M is $-\frac{16}{2.5}$ of the proton mass, ten times smaller than the coupling mass used in Ref. [21] so as to increase the coupling between the two anharmonic modes. The Morse parameters α_1 and α_2 are 2.175×10^8 cm^{-1} and the dissociation energies $D \equiv D_1 = D_2 = 5.52$ eV. This results in uncoupled Morse frequencies of $\omega_{g1} = \omega_{g2} = \alpha\sqrt{2D/m} = 7.2916 \times 10^{14}$ sec^{-1} (or 3868 cm^{-1}) each and 23 bound states per dimension. The frequencies of the excited electronic state described in (2.6) are typically lower than those in the ground state so that we used for ω_1 and ω_2 the value 1.4583×10^{14} sec^{-1} (or 774 cm^{-1}).

As mentioned in the previous section and as detailed in the Appendix, $\sigma(E)$ is defined as the mean energy interval between adjacent states. To average over a few states in a given energy interval one needs to use some multiple of it. We used for all the calculations 7 times the value of $\sigma(E)$ as defined by Eqs. (A.2) and (A.3).

The IC transition probability from the ground vibrational state ψ_{00} of the excited electronic state was computed as a function of the normalized energy gap $\Delta E/D$ for a positive shift $\Delta q = 0.7/\alpha$ in both degrees of freedom, using three different estimates: exact quantum diagonalization, zeroth order HK SCIVR for the quantum propagator as given by Eq. (2.14) and also a first order correction to the HK SCIVR as obtained from Eq. (2.19). For calculating the HK SCIVR we used a diagonal $\mathbf{\Gamma}$ matrix. We obtained best results by setting $\Gamma_{11} = \Gamma_{22} = m\omega_g/\hbar$, hence we used those values for our calculations.

We performed the integrals using the Monte Carlo method. 5×10^8 trajectories were used for the zeroth order integral defined in Eq. (2.14) obtaining an accuracy of 10^{-5} for the calculation of the IC transition probability. For the first order calculation defined by Eq. (2.19) many more trajectories were needed to obtain a similar accuracy. We used for the first order computations 2.5×10^{10} trajectories obtaining an accuracy of 5×10^{-6}. We do remark, that in any practical "on the fly" computation, one does not need such a high accuracy. Typically an error of 1 percent would be acceptable leading to sample sizes of the order of 10^3 which are amenable to "on the fly" computations.

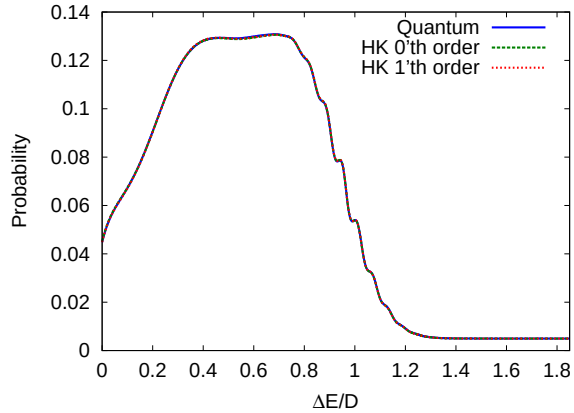

FIG. 2: (color online) Internal conversion transition probability vs. normalized energy gap $\Delta E/D$ for the decay of the ground vibrational state ψ_{00} of the excited electronic state. The shift between the minima of the ground and excited state potentials is taken to be $\Delta q = 0.7/\alpha$ in both dimensions. The comparison shown is between the exact quantum result, the 0'th order HK and the 1st order HK.

We evolved the overlap function defined in Eq. (2.11) up to a time of about 3 cycles of the basic frequency ω_g. As explained in section II.A, only a small part of this interval is needed when the transition energy is low (close to the bottom of the ground electronic state surface) but the full range is needed when the transition energy is high.

Results are shown in Figure 2 for a positive coordinate shift and the ground vibrational state in the excited electronic state. We find that the different estimates for the probabilities are hardly distinguishable. The semiclassical result is an excellent approximation to the exact quantum result.

To provide some more insight into the quality of the HK SCIVR dynamics, we plot in Figure 3 the differences between the numerically exact quantum results and those obtained with the zero-th order HK SCIVR method and the sum of the zero-th and first order HK SCIVR methods, shown in Figure 2. We note that the differences between the results are 2 to 3 orders of magnitude smaller than the results themselves. Also, the difference between the quantum and the first order HK results is smaller by 20% as compared to the difference between the quantum and the zeroth order HK. The perturbation theory thus corroborates that the zero-th order approximation is rather accurate. The same type of accuracy was also found for different shift parameter choices, and different initial conditions. Henceforth, we shall show only the result obtained using the zero-th order HK SCIVR methodology.

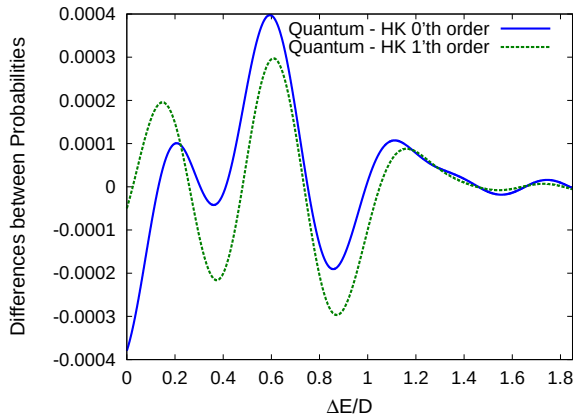

FIG. 3: (color online) Differences between the numerically exact quantum IC transition probability and the approximate probabilities as obtained using the HK 0th order and 0th plus 1st order HK SCIVR approximations.

B. Anharmonic effects

As noted in the Introduction, one may readily obtain analytic expressions for the IC transmission probability when the ground electronic state Hamiltonian is harmonic. It is thus of interest to probe how accurate the harmonic approximation really is. We will use in this section different shifts of the excited electronic state with respect to the ground electronic state, as shown in Fig. 4.

In panel (a) of Fig. 5 we plot the IC transition probability as a function of the (reduced) displacement energy $\Delta E/D$, for different initial vibrational states in the excited electronic state. The two potential curves are not shifted ($\Delta q = 0$), as shown in panel (a) of Fig. 4. It is note worthy that the transition probability maximizes when the energy shift is roughly half of the dissociation energy and then rapidly falls off. The same probabilities are plotted in panel (b) of the Figure but for the harmonic approximation of the potential, based on a harmonic expansion of the ground electronic state potential about its minimum. For low energy displacements, as might have been expected, the harmonic probabilities are very similar to the quantum. However, as the energy displacement increases, the anharmonicity kicks in. The harmonic probabilities remain relatively large even when the displacement energy is larger than the dissociation energy of the ground electronic state potential.

Displacing the two curves relative to each other creates an even more pronounced effect. In Fig. 6 we compare the IC transmission probability when the excited state potential minimum is displaced ($\Delta q = 0.7/\alpha$ for both degrees of freedom) toward the dissociative

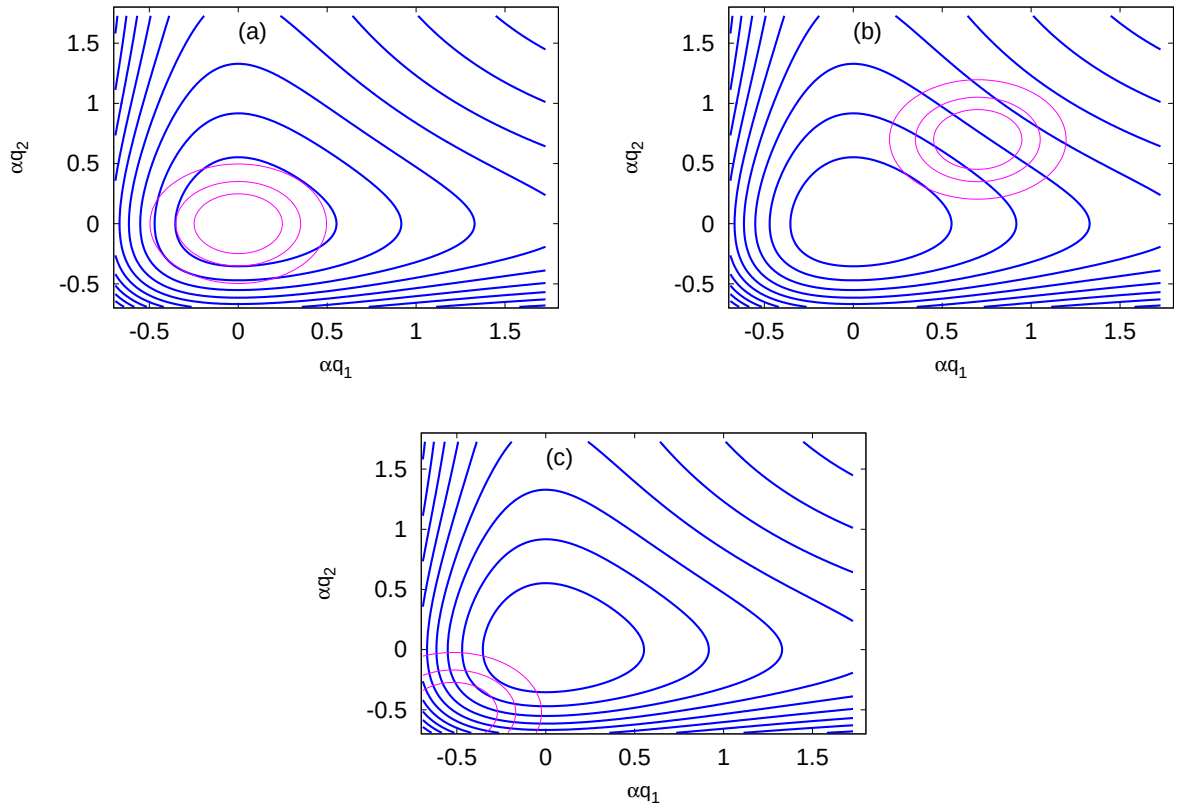

FIG. 4: (color online) Contour plot of the potentials. The ground electronic state contours are displayed as thick (blue) lines and the excited electronic state contours are displayed as thin (magenta) lines. Panel (a) shows a non shifted excited electronic state ($\Delta q = 0$), panel (b) shows the excited electronic state shifted toward the dissociation side (positive shift, ($\Delta q = 0.7/\alpha$)) in both dimensions, while panel (c) shows the excited electronic state shifted toward the repulsive side (negative shift, ($\Delta q = -0.52/\alpha$))) in both dimensions.

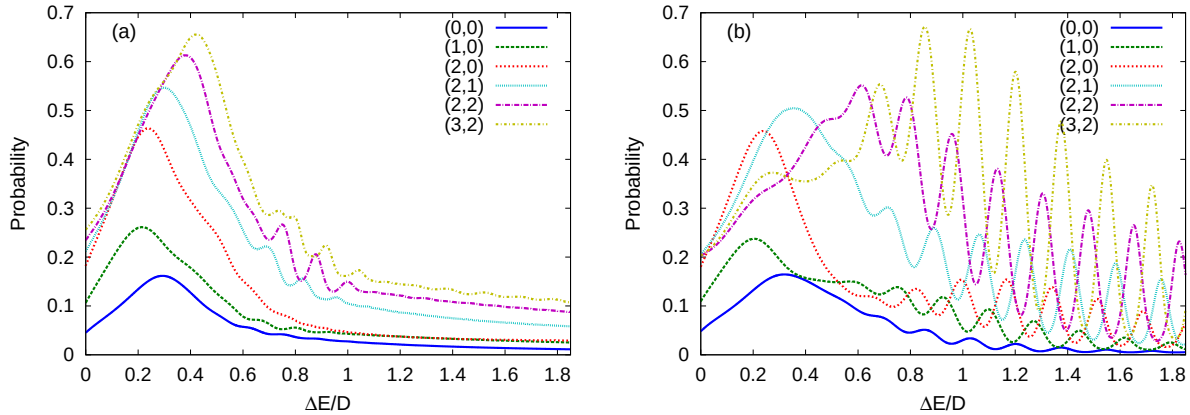

FIG. 5: (color online) The dependence of the IC transition probability on the normalized energy displacement $\Delta E/D$ for zero displacement ($\Delta q = 0$) and different initial excited states n, m. Panel (a) shows the HK SCIVR based results for the full anharmonic Hamiltonian, panel (b) shows the same for the harmonic approximation of the ground electronic state Hamiltonian.

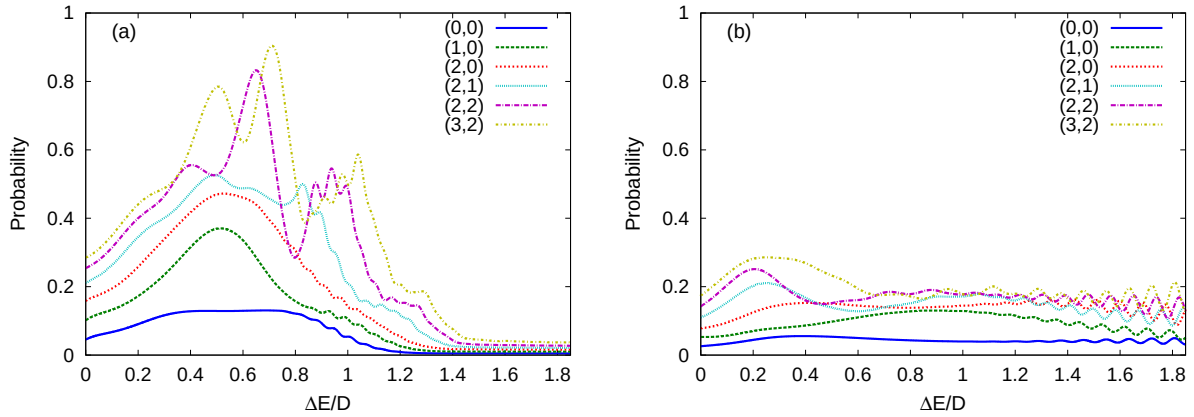

FIG. 6: (color online) The dependence of the IC transition probability on the normalized energy displacement $\Delta E/D$ for a fixed positive displacement of $0.7/\alpha$ and different initial excited states n, m. Panel (a) shows the HK SCIVR based results for the full anharmonic Hamiltonian, panel (b) shows the same for the harmonic approximation of the ground electronic state Hamiltonian.

side of the ground electronic state potential, as shown in panel (b) of Fig. 4. Panel (a) of Fig. 6 shows the HK SCIVR based results for the anharmonic ground state potential, while panel (b) shows the results based on the harmonic approximation to the ground electronic state Hamiltonian. One notes that in the presence of the anharmonicity, the transition probabilities for the different initial states maximize at shift energies which are at least half of the dissociation energy of the ground electronic state and then decay to almost zero for shift energies that are much higher than the dissociation energy. In contrast, the harmonic results remain rather constant throughout, with peak values that are much smaller, and they do not decay when the shift energy grows substantially beyond the dissociation energy.

We remark that when the two curves are displaced in configuration space, that even for low energy displacements the harmonic approximation fails, resulting in significantly lower IC transmission probabilities. This is due to the fact that the asymmetry in the potential causes the anharmonic wavefunction to be displaced away from the equilibrium point hence leading to a larger overlap with the excited state wavefunction. The opposite effect is observed when the configurational displacement is towards the repulsive side, as may be seen in Fig. 7. Here we compare the IC transmission probability, when the excited state potential minimum is displaced ($\Delta q = -0.52/\alpha$ for both degrees of freedom) toward the repulsive side of the ground electronic state potential, as shown in panel (c) of Fig. 4. Panel (a) of Fig. 7 shows the HK SCIVR based results for the anharmonic ground state potential, while panel (b) shows the results based on the harmonic approximation. Here,

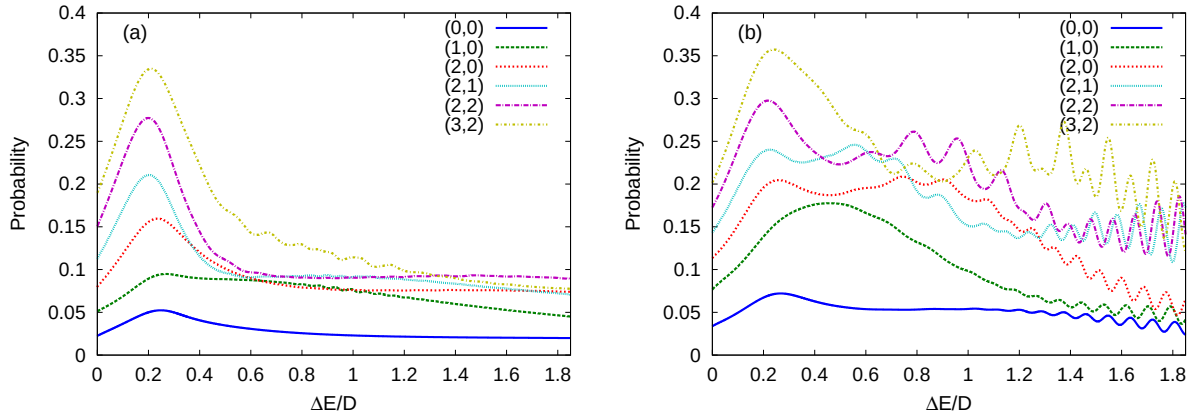

FIG. 7: (color online) The dependence of the IC transition probability on the normalized energy displacement $\Delta E/D$ for a fixed negative displacement of $-0.52/\alpha$ and different initial excited states n, m. Panel (a) shows the HK SCIVR based results for the full anharmonic Hamiltonian, panel (b) shows the same for the harmonic approximation of the ground electronic state Hamiltonian.

for low shift energies, the harmonic probability is somewhat higher, as explained above. At high displacement energies, the harmonic approximation again does not decay and so is a poor approximation to the anharmonic decay probabilities.

Perhaps the most striking feature in the three cases shown in Figs. 5-7 is that at energy shifts above the dissociation energy, the transmission probability decays, but the harmonic approximation does not. For the harmonic approximation of the ground state Hamiltonian there is no dissociative continuum. When the initial state mainly overlaps with the continuum oscillatory states, as especially seen in Fig. 6 then the overlap is small and the transition probability is small. If however one approximates the ground state Hamiltonian as a harmonic system, then one overlaps with localized bound states, and the effect of the shift energy is much weaker. Overall, especially at shift energies which are greater than half of the dissociation energy, the harmonic approximation fails and gives results which are typically much *larger* than those found with the full anharmonicity. Although the anharmonic density of states is higher than the harmonic, the central effect seems to be that at high shift energies, the harmonic wave functions remain relatively localized so that the overlaps are larger than those found for the full anharmonic case.

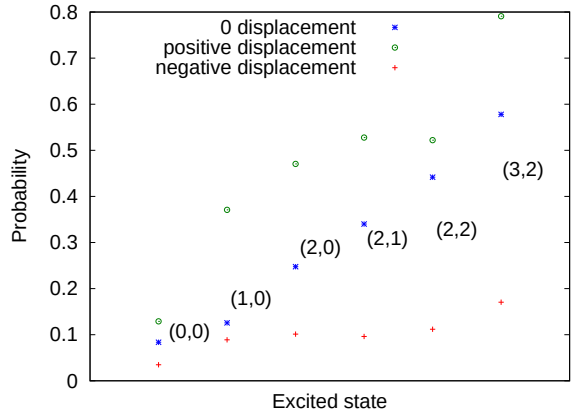

FIG. 8: (color online) Transition probabilities from different excited states (n, m), for a fixed energy gap of $0.5D$.

C. Initial state dependence of the transmission probability

Experimentally, it has been established [10, 16, 24, 25] that the IC transmission rate increases as the energy of the initial state increases. Qualitatively, as the initial energy increases, so does the density of states in the ground electronic state and so the overlap grows. That this is indeed the case is shown in Fig. 8 where we plot the transmission probability for a fixed value of the shift energy (chosen to be 0.5 of the dissociation energy) for positive, zero and negative displacement of the two electronic curves. One notes, that indeed, irrespective of the coordinate shift between the two electronic states, the IC transmission probability increases with increasing initial state, reflecting the increase in the density of states of the ground state vibrations.

D. Coupling effects

One way of overcoming the limitation to harmonic systems is by ignoring the coupling between modes. It is easier to compute the internal conversion probability when the system is separable. We find that increasing the displacement of the excited electronic toward the dissociative side, increases the effect of coupling. Panel (a) of Fig. 9 shows the IC transmission probability when the excited electronic state potential minimum is displaced by $\Delta q = 0.7/\alpha$ in both degrees of freedom, but without the coupling term in the ground electronic state Hamiltonian, while panel (b) shows the differences between the uncoupled results and the parallel coupled results from panel (a) of Fig. 6. Clearly, the IC transition

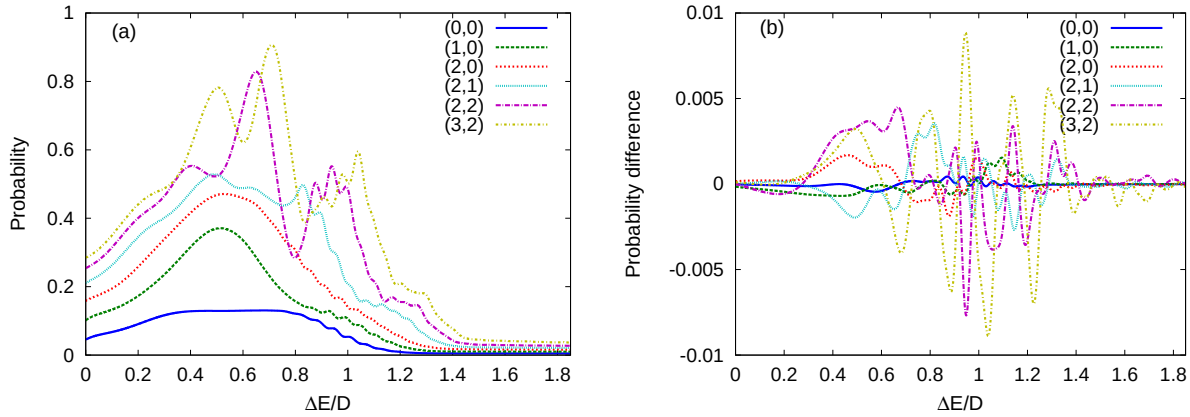

FIG. 9: (color online) Panel (a) shows the HK SCIVR based results for the dependence of the IC transition probability on the normalized energy displacement $\Delta E/D$ for positive displacement ($\Delta q = 0.7/\alpha$) and different initial excited states n, m, for the anharmonic uncoupled ground Hamiltonian. Panel (b) shows the differences between the coupled and the uncoupled results, all other parameters being identical.

probability for the model Hamiltonian used in the present study is only weakly dependent on the coupling between the modes.

IV. CONCLUDING REMARKS

We have shown that the internal conversion transition probability can be calculated accurately with the HK SCIVR method. The first order correction to the semiclassical approximation is small. The accuracy was also verified by comparing the SCIVR estimates with the numerically exact quantum mechanical results. This is encouraging, as it would justify the use of the HK SCIVR method for the study of internal conversion in larger systems. Perhaps not less important is the observation that a harmonic approximation is not very reliable, giving qualitatively incorrect results especially at energies in the vicinity of the dissociation energy of the ground electronic state potential.

The results presented here are in qualitative agreement with experimental observations [10, 16, 24, 25] on the dependence of IC rates on the initial excited state for formaldehyde. As in the experiments, we find the general tendency of higher internal conversion transition probability, for higher initial states of the excited electronic state.

These computations imply that the HK SCIVR method is a good candidate for implementation in "on the fly" computation of IC rates for systems with many degrees of freedom.

Perhaps the greatest challenge facing the HK SCIVR method is that the computation of the prefactor depends on the computation of the Hessian matrix "on the fly". This can become quite expensive. In this context we mention that there are available methods for simplifying the computation, as discussed for example in Ref. [33].

Acknowledgments

This work has been supported by grants from the Israel Science Foundation and the German-Israeli Foundation for Scientific Research and Development.

Appendix A: The coarse grained level spacing

In this appendix we describe how we evaluated the coarse grained energy dependent level spacing function $\sigma(E)$. The number of states up to an energy E between 0 and the dissociation energy D is defined as:

$$N(E) = \mathrm{Tr}[\theta(E - H_g)]. \tag{A.1}$$

For energies in the interval $D < E < 2D$ there are bound and unbound states, hence N is infinite for energies higher than the dissociation energy. By numerically diagonalizing the ground state (anharmonic and coupled modes) Hamiltonian, we could get the (staircase like) function $N(E)$. We then fit the staircase function to a continuous function of the form:

$$N_{an}(E) = \frac{1}{2}\left[\left(\frac{E}{\hbar\omega_g}\right)^2 + \frac{E}{\hbar\omega_g}\right] - 0.01\left(\frac{E}{\hbar\omega_g}\right)^3 + 0.0032\left(\frac{E}{\hbar\omega_g}\right)^4. \tag{A.2}$$

A comparison between the numerically exact staircase function and its continuous fit is shown in Fig. 10.

The energy interval function is then by definition

$$\sigma(E) = dE/dN \tag{A.3}$$

calculated from (A.2), for energies between 0 and D. For energies between D and $2D$, because of the mixing of bound and unbound states we used the value of $\sigma(D)$. For comparisons with the harmonic approximation to the ground state potential we used only the

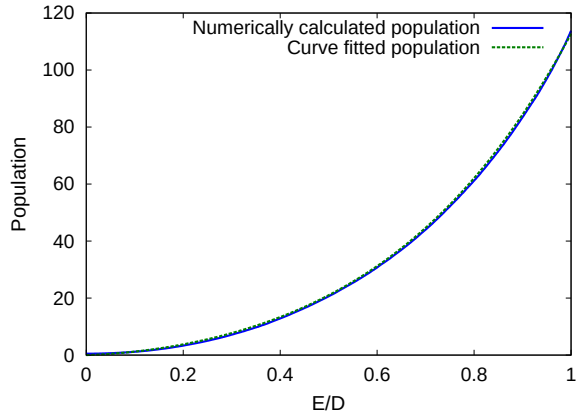

FIG. 10: (color online) Two dimensional coupled Morse population plotted as a function of the dimensionless energy E/D. We compare the fitted function as obtained from Eq. A.2 with the numerically exact staircase function obtained by numerically diagonalizing the Hamiltonian of the ground electronic state. The deviation of the fitted function from the exact function is less than 2% for $E/D > 0.45$

first 2 terms in (A.2).

---

[1] G.W. Robinson and R.P. Frosch, J. Chem. Phys. **37**, 1962 (1962).

[2] G.W. Robinson and R.P. Frosch, J. Chem. Phys. **38**, 1187 (1963).

[3] S.H. Lin, J. Chem. Phys. **47**, 3759 (1966).

[4] S.H. Lin and R. Bersohn, J. Chem. Phys. **48**, 2732 (1968).

[5] S.H. Lin, C.H. Chang, K.K. Liang, R. Chang, J.M. Zhang, T.-S. Yang, M. Hayashi, Y.J. Shiu, and F.C. Hsu, Adv. Chem. Phys. **121**, 1 (2002).

[6] Q. Peng, Y.P. Yi, Z.G. Shuai and J. Shao, J. Chem. Phys. **126**, 114302 (2007).

[7] Q. Peng, Y.P. Yi, Z.G. Shuai and J. Shao, J. Am. Chem. Soc. **129**, 9333 (2007).

[8] Q. Peng, Y. Niu, C. Deng and Z. Shuai, Chem. Phys. **370**, 215 (2010).

[9] M. Etinski, J. Tatchen and C.M. Marian, J. Chem. Phys. **144**, 154105 (2011).

[10] E. S. Yeung and C. B. Moore, J. Chem. Phys., **60**, 2139 (1974).

[11] H. Wang, C. Zhu, j.-G. Yu and S.H. Lin, J. Phys. Chem. A **113**, 14407 (2009).

[12] R. He, L. Yang, C. Zhu, M. Yamaki, Y.-P. Lee and S.H. Lin, J. Chem. Phys. **134**, 094313 (2011).

[13] For recent reviews and applications see the book "Multidimensional Quantum Dynamics:

MCTDH Theory and Applications" edited by H.-D. Meyer, F. Gatti, and G. A. Worth (Wiley VCH, 2009).

[14] W.H. Miller, J. Phys. Chem. A **105**, 2942 (2001).

[15] M. F. Herman and E. Kluk, J. Chem. Phys. **91**, 27 (1984).

[16] W. E. Henke, H. L. Selzle, T. R. Hays, E. W. Schlag and S.H. Lin, J. Chem. Phys., **76**, 1327 (1982).

[17] J. K. Frisoli, W. F. Polik and C. B. Moore, J. Phys. Chem. **92**, 5417 (1988).

[18] S. Zhang and E. Pollak, Phys. Rev. Lett. **91**, 190201 (2003).

[19] S. Zhang and E. Pollak, J. Chem. Phys. **119**, 11058 (2003).

[20] S. Fischer, J. Chem. Phys. **53**, 3195 (1970).

[21] E. L. Sibert, J. T. Hynes and W. P. Reinhardt, J. Chem. Phys. **77**, 3595 (1982).

[22] K. Stefanski and E. Pollak, J. Chem. Phys. **87**, 1079 (1987).

[23] E. Pollak and J. Shao, J. Phys. Chem. A **107**, 7112 (2003).

[24] C. S. Parmenter, Adv. Chem. Phys. **22**, 365 (1972).

[25] E. Evans. D. Heller, S. A. Rice and R. Scheps, Trans. Farad. Soc. II **69**, 856 (1973).

[26] W. H. Green, C. B. Moore, W. F. Polik, *Annu. Rev. Phys. Chem*, **43**, 591 (1992).

[27] J. M. Millam, V. Bakken, W. Chen, W. L. Hase, H. B. Schlegel, *J. Chem. Phys.*, **111 (9)**, 3800 (1999).

[28] D. Townsend, S. A. Lahankar, S. K. Lee, S. D. Chambreau, A. G. Suits, X. Zhang, J. Rheinecker, *Science*, **306**, 1158 (2004).

[29] S. Matsika *J. Phys. Chem. A*, **108**, 7584, (2004).

[30] J. V. Van Vleck, *Proc. Nat. Acad. Sci. USA* **14**, 178 (1928).

[31] W.H. Miller, *J. Mol. Phy.*, **100 (4)**, 397 (2002).

[32] V.I. Filinov, *J. Nucl. Phys. B*, **271**, 717, (1986).

[33] J. Tatchen, E. Pollak, G. Tao and W.H. Miller, J. Chem. Phys. **134** 134104 (2011).